Appl. Phys. B (2003)
DOI: 10.1007/s00340-003-1299-z

Applied Physics B
Lasers and Optics

J. ALNIS*
B. ANDERSON**
M. SJÖHOLM
G. SOMESFALEAN
S. SVANBERG✉

Laser spectroscopy of free molecular oxygen dispersed in wood materials

Department of Physics, Lund Institute of Technology, P.O. Box 118, 22100 Lund, Sweden

Received: 29 January 2003/Revised version: 21 July 2003
Published online: 30 September 2003 •

ABSTRACT The recently introduced **Ga**s in **S**cattering **M**edia **A**bsorption **S**pectroscopy (GASMAS) technique is applied to the study of various wood samples. Molecular oxygen in the pores of the strongly scattering material is detected using diode laser spectroscopy around 760 nm. Diffuse light propagation in these media is studied by time-dispersion measurements. Furthermore, anisotropy related to the fibre structure of wood and gas diffusion properties are studied. Promising extensions of the experiments are discussed.

PACS 42.55.Px; 42.62.Fi; 81.05.Rm; 81.70.Fy; 87.64.Cc

1 Introduction

Solid-state and liquid materials exhibit only broad features in optical absorption spectroscopy due to the complex interaction of the atoms. Thus, the requirements for resolution in spectroscopic instrumentation are moderate in the study of such materials. On the other hand, many natural and artificial materials contain pores filled with gas, for which the associated absorptive signals are typically 10^4 times narrower, rendering them invisible in standard spectroscopy of solids and liquids. However, by using single-mode diode laser radiation combined with modulation techniques [1], even very weak and narrow gas absorption signals in open air can be retrieved. Recently, we demonstrated the first measurements with the **Ga**s in **S**cattering **M**edia **A**bsorption **S**pectroscopy (GASMAS) technique [2] of gas embedded in porous media. In our first demonstrations, atmospheric oxygen was monitored in samples as diverse as wheat flour, polystyrene foam, and apple. Diode laser spectroscopy combined with sensitive modulation techniques was performed on an A-band line around 760 nm. Gas diffusion in polystyrene was studied by first placing the sample in pure nitrogen for several hours and subsequently observing the time constant for the re-invasion of the ambient air into the material.

✉ Fax: +46-46/2224250, E-mail: Sune.Svanberg@fysik.lth.se
*_Permanent address_: Institute of Atomic Physics and Spectroscopy, University of Latvia, 19 Rainis Blvd., Riga LV-1586, Latvia
**_Permanent address_: Laser and Fibre Optics Centre, University of Cape Coast, Cape Coast, Ghana

A porous medium by nature scatters light, resulting in many different trajectories for the photons penetrating a sample. Thus, absorption experiments cannot be evaluated by a straightforward use of the customary Beer–Lambert law. Instead diffuse light propagation as encountered in tissue or cloud optics has to be considered. Concentration determination requires the effective path length through the medium to be known, an aspect that has been addressed in [3], where experimental techniques and theoretical approaches well known in the field of medical tissue optics [4–6] were employed. The distribution of short and long path lengths could be determined in time-resolved transillumination measurements and verified in continuous-wave experiments, in which the distance between the points of light injection into the sample and the photon pick-up by the receiver was altered.

Further aspects of the GASMAS technique are explored in the present paper, which focuses on gas in an important class of porous natural materials, wood, which has been addressed by others, although using intrusive methods (see, e.g. [7]). As in previous work, we restrict our gas studies to molecular oxygen, and use a diode laser source, although virtually any gas within the reach of tunable lasers with narrow enough linewidths can be used. The experimental arrangements and the measurement techniques presently used are briefly described in the next section. Then, measurements are described in Sect. 3, where a comparative study of eight different types of common woods is performed, and a study of the anisotropy induced by the orientation of the annual rings is presented. Air diffusion into wood is also elucidated, showing differences between wood of different types. Finally, a concluding section discusses the results and suggests some extensions to the techniques.

2 Experimental arrangements and procedures

2.1 *Continuous wave GASMAS spectroscopy*

The experimental setup for GASMAS, shown schematically in Fig. 1a, has been described in detail elsewhere [2, 3]. The diode laser and the lens that coupled light into the fibre were placed in an enclosure flushed with nitrogen to eliminate oxygen from the ambient air. A 600-μm fibre was used to bring the probe light via a collimating lens to the sample, which was illuminated with a 3-mm-diameter beam. In order to obtain a high photon collecting efficiency

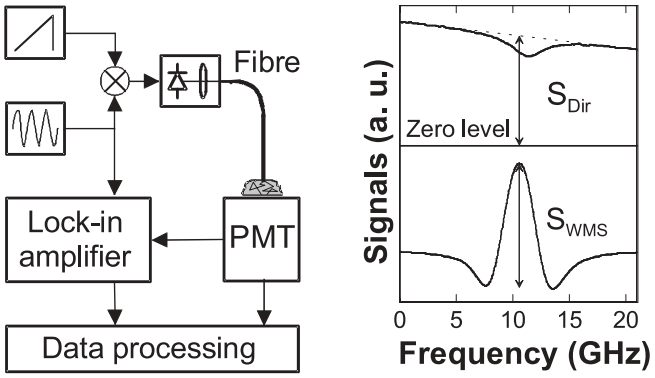

FIGURE 1 **a** Schematic of the GASMAS setup. **b** WMS signal of oxygen recorded for a 10-m column of air and corresponding pure absorptive imprint

and a high dynamic range, the sample was placed directly on a photomultiplier tube (PMT; EMI9558 QA) cathode, which was protected from visible light by a blocking coloured glass filter (Schott RG695).

A diode laser (Sharp LT031MDO) with an output power of 7 mW was temperature tuned to the molecular oxygen line at 761.003 nm (R7R7 of the A-band). The laser injection current was swept at a repetition frequency of 4 Hz, allowing a linear scan over the absorption line. A 55-kHz sine-wave modulation was superimposed on the current ramp, and the absorption signal was detected by the use of a lock-in amplifier (EG&G Princeton Applied Research 5209) at the second harmonic of this modulation frequency, rendering a wavelength modulation spectroscopy (WMS) signal that was similar to the second derivative of the absorption profile. Signal averaging, of between 32 and 1024 scans depending on the level of noise, was performed on a computer-controlled digital oscilloscope. The maximum wavelength drift was less than 500 MHz/h. Thus, with a pressure-broadened oxygen linewidth of about 3.5 GHz at ambient pressure, the drift of the laser wavelength was negligible even during substantial averaging.

The wavelength modulation spectroscopy (WMS) signal of the absorbing oxygen in a 10-m column of air and the corresponding pure absorptive imprint are shown in Fig. 1b. The slight asymmetry of the WMS signal was caused by a variation of the modulation depth during the laser scan. The peak-to-peak value of the signal (S_{WMS}) was, in the absorption regime explored, linearly proportional to the gas-related differential absorption and to the light intensity reaching the detector. Hence the WMS signal was always normalised by dividing it by the interpolated light intensity at the peak absorption wavelength (S_{Dir}). The optical densities of the samples varied by several orders of magnitude and so did the light levels reaching the detector. The PMT gain was adjusted by changing the supply voltage to achieve high amplification and linearity in the detected signal. Clearly, oxygen concentration measurements in optically dense samples have less sensitivity because the weak signals vanish in the noise. In this case in particular, enhanced accuracy can be achieved by first performing a least squares linear fitting of an ideal WMS curve to the noisy recorded WMS curve. Thus, instead of directly using the peak-to-peak value of the noisy curve, the corresponding fitting factor constitutes a measure of the gas absorption. One simple method for obtaining the ideal WMS curve is to use an experimental curve recorded with a good signal-to-noise ratio.

It could be checked that no spurious oxygen signal occurred and that the flushing with nitrogen of the diode laser chamber was adequate by replacing the sample with an appropriate absorptive filter, which attenuated the transmitted light to a level that could be detected linearly by the PMT, and by ensuring that there was no air gap between the filter and the collimator.

The oxygen concentration in the sample could be related to the oxygen in the ambient air by deliberately introducing an air gap between the fibre collimator and the sample (the standard addition method of analytical chemistry). The WMS signal, normalised to the intensity detected, could, in the regime of low absorption, be considered to be linear with the absorption path length.

2.2 *Time-resolved photon propagation spectroscopy*

The setup used for time-resolved measurements of photon path lengths in wood samples has been described previously [3] and is shown schematically in Fig. 2a. A 760-nm laser diode (Mitsubishi ML 4405) was used to generate short pulses having an average optical power of 0.3 mW at a 10-MHz repetition rate. Light from the laser was passed through a 600-μm-thick optical fibre to one side of the sample and another similar fibre collected light on the opposite side and conveyed it to a cooled PMT (Hamamatsu R2566U-07). Part of the laser output was divided by a beamsplitter into a reference fibre coupled directly to the PMT to provide a time fiducial. The response function of the detection system, assessed by the use of sub-picosecond laser pulses, had a full width at half maximum of 60 ps. When using the diode laser, the corresponding width was found to be 140 ps.

A recorded photon distribution after passage through a 9-mm-thick sample of Portuguese marble, and the reference pulse, are shown in Fig. 2b. There were essentially no photons that got through the material directly (ballistic photons), and there were only a few photons that exited the sample very late because many were absorbed or scattered in the material. The evaluation of the photon mean path length in the mate-

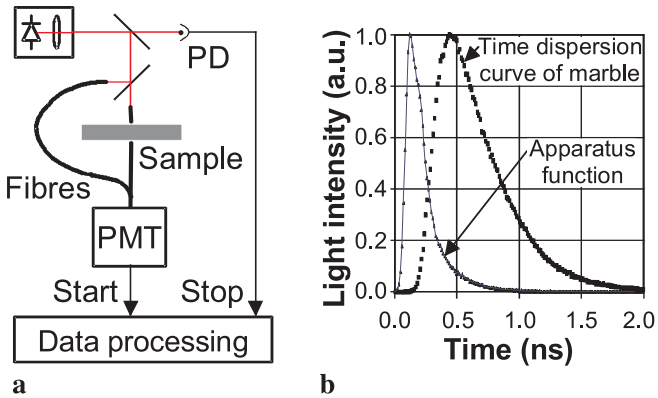

FIGURE 2 **a** Schematic of the time-resolved measurement setup. **b** Photon distribution after transillumination of a 9-mm-thick slab of marble. The apparatus function is also included for the pulse only

rial requires an estimate of the effective index of refraction of the material, i.e. the local light velocity. Assuming that the mean light velocity in the sample is 2/3 the velocity of light, close to the values for glass and water, we note that 1 ns corresponds to 200 mm in the sample. For the 9-mm-thick sample illustrated, it is obvious that the mean photon path length was several times longer than the geometrical distance between the injection and detection fibres, emphasising the important role of scattering. For the natural samples we studied in the present investigation, the scattered photon distribution was only a few times broader than the apparatus function. In this case, the mean photon dwell time in the material can be obtained by a deconvolution of the apparatus function from the measured temporal distribution.

The linewidth of the pulsed laser is much larger than the absorption linewidth of the gas, and for the case of oxygen the differential absorption due to gas in the sample is less than a few percent. Thus, when studying the time delay and attenuation of light pulses in the bulk material, it does not matter whether the laser is tuned to the oxygen absorption line or not. However, the scattering properties are strongly wavelength dependent, meaning that the continuous wave and time-resolved measurements should be performed at approximately the same wavelength.

3 Measurements and results

Basic measurements of different aspects related to light propagation and embedded gas in wood were performed. By shining light through the samples and adding known distances of ambient air, the gas content in the porous samples could be expressed as an equivalent mean path length, that is, the path length in air rendering the same absorption as the encountered oxygen in the material. First, measurements of 6-mm-thick slabs of wood of different species and different densities were performed. In Fig. 3, the equivalent mean path lengths of oxygen in eight different types of wood are plotted versus the density of the material (ten different densities). The different species are listed in the figure caption. The annual rings in the measured samples had a uniform inclination of approximately 45° to the primary impinging laser beam. Each sample was measured at three different points, and at each point three different averages consisting of 512 individual scans were acquired using a circular detection area with a diameter of 25 mm. The error bars indicated correspond to ± 2 standard deviations. Note that the density of wood is an average of the whole sample, and that there could be local variations within the sample. However, it can clearly be seen that with increasing wood density the oxygen absorption decreased. Clearly the signal depends on both the gas content and the light transport properties (i.e. the effective path length) of the material. Measurements were also performed on denser species, Pear, Norway Maple, Beech, Pedunculate Oak, Wych Elm, Wild Cherry and Hornbeam, but the emerging light intensities were too low and consequently the gas absorption signals too noisy with the present detection system. The most optically dense sample that still gave a measurable gas absorption signal was that of Ash (see curve 8 in Fig. 3b).

The orientation of the annual rings relative to the direction of the impinging light could be anticipated to influence

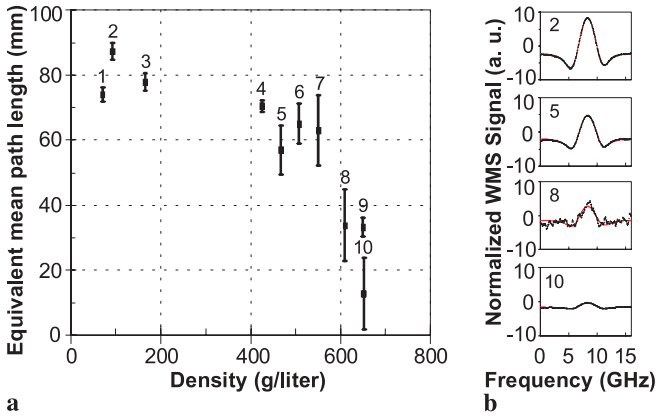

FIGURE 3 **a** Equivalent mean path lengths of oxygen for eight different types of wood plotted versus the density of the material. The annual rings in the measured samples had an inclination of approximately 45° to the primary impinging laser beam. Data are given for Balsa (*Ochroma pyramidale*, *curves 1–3*), Norway Spruce (*Picea abies*, *curve 4*), European Larch (*Larix decidua*, *curve 5*), Alder (*Alnus glutinosa*, *curve 6*), Aspen (*Populus tremula*, *curve 7*), Ash (*Fraxinus excelsior*, *curve 8*), Birch (*Betula sp.*, *curve 9*), and Scots Pine (*Pinus sylvestris*, *curve 10*). **b** Corresponding WMS signals for some of the samples together with fitted waveforms

the light transport. Therefore, the inherent anisotropy of wood was investigated using cubes of 15-mm side length. The oxygen light absorption and the light transmission were measured through a cube of Norway Spruce wood (*Picea abies*) ($\varrho = 387\ \mathrm{g/dm^3}$), letting the laser beam enter in the three different principal directions (radially through the annual rings, longitudinally along the annual rings along the stem, and tangentially along the annual ring layers, respectively). The results are presented in Fig. 4. Each principal direction was measured from both sides, and on each side three different averages consisting of 512 individual scans were acquired using a circular detection area with a diameter of 6 mm. The error bars indicate the 95% confidence interval and it can be seen that the spread in, as well as the level of, gas absorption measured increased with decreasing amount of light transmitted.

The same measurements were also performed on a similar cube of Scots Pine (*Pinus sylvestris*) ($\varrho = 668\ \mathrm{g/dm^3}$), rendering the same relative difference between the three orientations but with equivalent mean path lengths approximately half the corresponding values for the less dense cube. The lowest gas absorption, and the highest light transmission, was found for the case in which the light was guided along the fibres, that is, when the light path in the wood was shortest.

In the measurements presented in Figs. 3 and 4 it can be seen that the equivalent mean path lengths were about one order of magnitude longer than the geometric distance between the points of light injection and detection. Since wood obviously contains a smaller fraction of oxygen than the ambient air, the distance travelled by the light inside the material is even longer than that. This fact is highlighted in Fig. 5, in which a time dispersion curve recorded for a 6-mm-thick slab of Ash wood (*Fraxinus excelsior*), with annual rings at an inclination of about 45° to the primary impinging laser beam, is displayed.

Dynamic processes related to gas diffusion in wood were also investigated, by measuring the light absorption of oxygen in samples of wood directly after they were brought out into

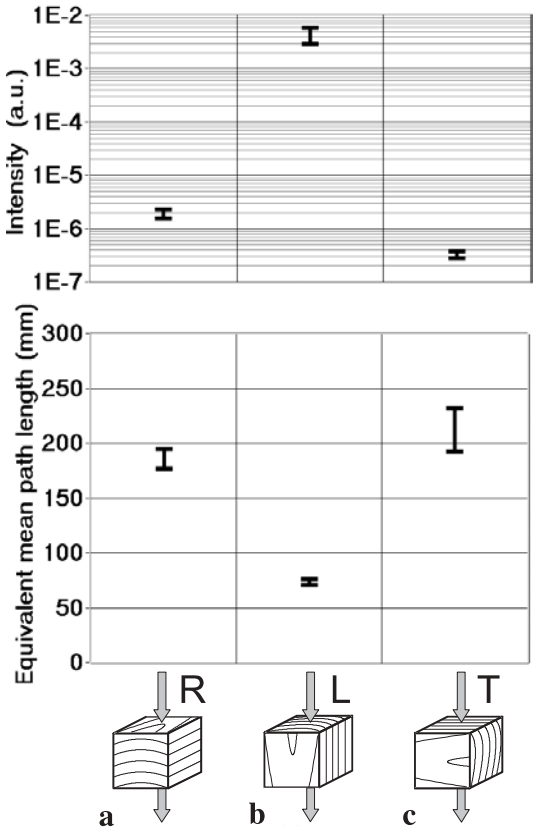

FIGURE 4 Light transmission (*upper part*) and oxygen absorption (*lower part*) measurements through a cube (side 15 mm) of Norway Spruce wood **a** radially through the annual rings, **b** longitudinally along the annual rings along the stem, and **c** tangentially along the annual ring layers

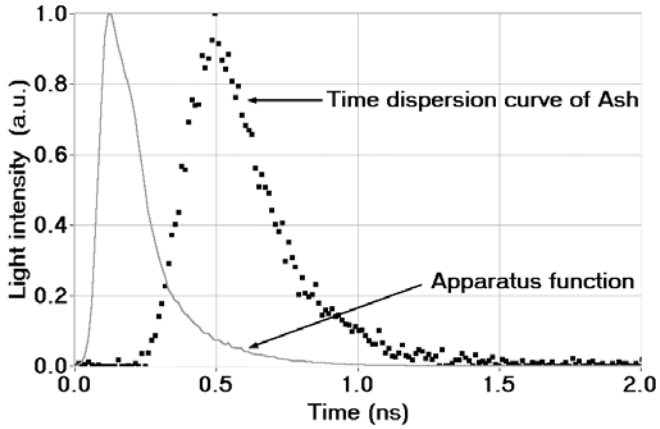

FIGURE 5 Time dispersion curve recorded for a 6-mm-thick sample of Ash wood (*Fraxinus excelsior*). The apparatus function is also included for the pulse only

ambient air from an environment of pure nitrogen. As shown in Fig. 6, the period of previous oxygen-free storage affected the amount of gas exchanged in the sample; the signal started from a lower level for longer periods in the oxygen-free environment. However, the time constant of re-invasion seemed not to be affected by the length of the pre-treatment, and was found to be approximately three hours. The curves presented were measured on the same 10-mm-thick slab of Balsa wood (*Ochroma pyramidale*) ($\varrho = 71\ \mathrm{g/dm^3}$) using a circular detection area with a diameter of 25 mm. Each data point was

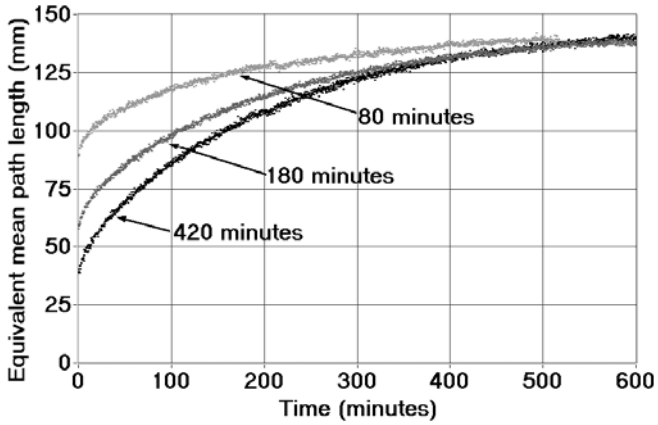

FIGURE 6 Recordings of the diffusion of oxygen into the same 10-mm-thick sample of Balsa wood that had been stored in a pure nitrogen atmosphere for different times, as indicated in the figure

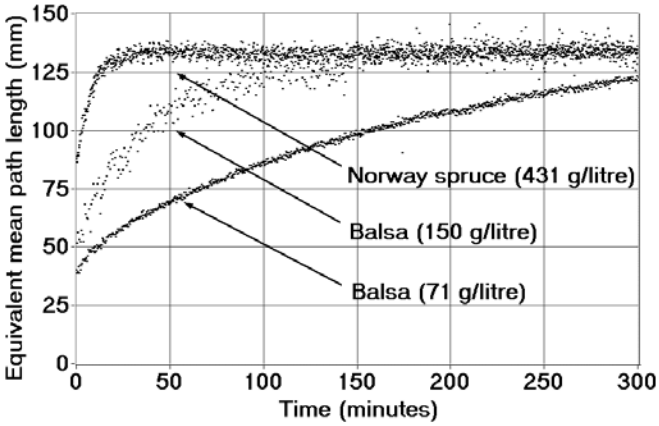

FIGURE 7 Recordings of the diffusion of oxygen into 10-mm-thick samples of Norway Spruce ($\varrho = 431\ \mathrm{g/dm^3}$), Balsa ($\varrho = 150\ \mathrm{g/dm^3}$), and Balsa ($\varrho = 71\ \mathrm{g/dm^3}$)

obtained by averaging 64 individual scans on the oscilloscope, an integration time of 16 s.

Further measurements revealed that the time scale of gas re-invasion was different in different samples of wood. In Fig. 7, the diffusion of oxygen into 10-mm-thick slabs of Norway Spruce ($\varrho = 431\ \mathrm{g/dm^3}$), Balsa ($\varrho = 150\ \mathrm{g/dm^3}$), and Balsa ($\varrho = 71\ \mathrm{g/dm^3}$) are presented. Somewhat unexpectedly, the gas penetration was found to be fastest in the densest material. It was observed that both long and short time constants govern the gas transport. It seems that gas spreads quickly through coarser structures, while penetration through the cell walls of the balsa wood was slow. For long times the equivalent mean path length approached an equivalent mean path length that was longer than that in Fig. 3, in which a thickness of 6 mm was used instead of one of 10 mm.

Gas absorption measurements were also performed on marble. However, with the present setup, it was not possible to unambiguously assign the oxygen signal to air inside the sample, due to the very low amount of enclosed gas.

4 Discussion and conclusions

The GASMAS technique provides new opportunities for studying gas enclosures in natural and synthetic

materials. The present study illustrates different aspects of the technique used in the investigation of wood of different kinds. Different species of wood yield widely differing integrated oxygen signals, which are shown to have a relation to the mass density of the wood. The annual ring structure leads to strong signal anisotropy due to differences in light transport. A determination of the gas concentration in materials is possible in principle, as shown in our earlier work [3], but requires a combination of GASMAS data and data obtained in temporally resolved measurements for assessing the mean optical path length. In this way, a generalised Beer–Lambert relation can again be established in the spectroscopy of gas in porous media. However, obtaining accurate values for the index of refraction (i.e. the velocity of light) in the studied materials is particularly difficult. Another aspect that calls for further investigation is the relative distribution of light between the solid phase and the gas phase of the scattering media.

On the other hand, the concentration ratios of gases, and in particular, changes in concentration ratios, can readily be determined if the same approximate wavelength is used for the absorption lines of the two species, so that the same scattering conditions prevail. This scheme can be of particular importance for the study of, for example, physiological processes in plants.

Measurements of the GASMAS type can be an important tool for analysing the gas diffusion properties of porous materials. By monitoring the rate at which atmospheric oxygen re-invades a sample previously exposed to a different ambient atmosphere, such as nitrogen, diffusion coefficients can be evaluated [8]. Gas transport studies using the GASMAS technique are also expected to be useful in studies of gas absorption in, for example, catalysts embedded in zeolites.

Although diffusion in wood was addressed in this paper, we will also mention several related possibilities of considerable practical interest.

Wood, wood-chip, and gypsum boards are important building and construction materials, which are most frequently covered with paints for protection and aesthetic reasons. The varying gas exchange related to different types of paints can be assessed by the present technique. Of particular interest is water vapour and water, with building damage due to moisture being a major consideration. For low levels of moisture, the gaseous water in the pores can be studied (a saturation clearly occurs for higher levels), while for high levels, liquid water replacing the gas in the pores can also be studied in an indirect way, since it will depress the oxygen signal [9]. The related effects due to scattering suppression by the presence of an index-matching fluid have to be elucidated.

Marble and other porous stone materials used in the construction of historical buildings and sculptures suffer damage due to weather exposure, particularly when combined with increasing levels of atmospheric pollutants. Protective surface coatings, which are ideally invisible, are therefore being introduced. Due to the strongly differing properties of the coating and the stone, fluorescence techniques are a powerful tool for detecting such coatings [10]. Recently the Lund group participated with its mobile lidar system in the remote fluorescence imaging of the Parma Cathedral and Baptistery, with spectacular manifestations of facade treatments [11]. GASMAS measurements on untreated and treated surfaces of porous stone might help to elucidate the functioning of the protective coatings in a similar way to that discussed for studies of painted wood. The concentration of oxygen in porous marbles can be expected to be much lower than in wood, but sensitive equipment should be able to pick up the relevant signals.

In the preservation of foodstuffs it is important to keep atmospheric oxygen away, which is frequently accomplished by using plastic films or laminates. This is the case with, for example, meats packaging, where the film also has the additional purpose of preventing drying out and bacterial access. Related techniques are used for beverages, especially milk. It can be anticipated that the GASMAS technique will also find applications in these contexts.

In conclusion, the GASMAS technique opens up many new diagnostic and analytical possibilities, some of which have been experimentally demonstrated in the present paper, while others could be addressed in further investigations.

ACKNOWLEDGEMENTS The authors are grateful to Mr.O. Marcillo for assistance in some of the measurements. This work was supported by the Swedish Research Council, the International Programme in the Physical Sciences (Uppsala), the Swedish Institute (Visby Programme), and the Knut and Alice Wallenberg Foundation.

REFERENCES

1 M. Kroll, J.A. McClintok, O. Ollinger: Appl. Phys. Lett. **51**, 1465 (1987)
2 M. Sjöholm, G. Somesfalean, J. Alnis, S. Andersson-Engels, S. Svanberg: Opt. Lett. **26**, 16 (2001)
3 G. Somesfalean, M. Sjöholm, J. Alnis, C. Klinteberg, S. Andersson-Engels, S. Svanberg: Appl. Opt. **41**, 3538 (2002)
4 S.R. Arridge, M. Cope, D.T. Delpy: Phys. Med. Biol. **37**, 1531 (1992)
5 T.J. Farrell, M.S. Pattersson, B. Wilson: Med. Phys. **19**, 879 (1992)
6 G. Müller, B. Chance, R. Alfano, S. Arridge, J. Beuthan, E. Gratton, M. Kaschke, B. Masters, S. Svanberg, P. van der Zee (Eds.): *Medical Optical Tomography: Functional Imaging and Monitoring* (SPIE, Bellingham 1993)
7 D. Gansert, M. Burgdorf, R. Lösch: Plant Cell Env. **24**, 1055 (2001)
8 M. Sjöholm: 'Determination of Gas Diffusion Coefficients Using the GASMAS Technique', to appear
9 S. Svanberg, M. Sjöholm, G. Somesfalean: Method and Device for Investigation of a Surface Layer, Patent application PCT/SE03/00717 (2003)
10 G. Ballerini, S. Bracci, L. Pantani, P. Tiano: Opt. Eng. **40**, 1579 (2001)
11 D. Lognoli, G. Cecchi, I. Mochi, L. Pantani, V. Raimondi, R. Chiari, T. Johansson, P. Weibring, H. Edner, S. Svanberg: Appl. Phys. B **76**, 1 (2003)